CHAPTER II
LITERATURE REVIEW

2.1 Petroleum Crude Oil

Petroleum crude oil is the complex mixture of hydrocarbon compounds containing physically and chemically difference in properties. The petroleum crude oil can be classified based on difference in solubility and polarity into 4 major fractions: saturates, aromatics, resins, and asphaltenes (SARA). In laboratory, asphaltenes are initially precipitated out of crude oil by adding n-alkanes as precipitant and the remaining solution is named maltenes. Maltenes is further absorbed on silica or alumina absorbents and eluted by solvents with different polarity to sequentially separate saturates, aromatics and resins (Speight, 1999).

2.2 Asphaltenes

Asphaltenes are dark brown to black friable solids with no definite melting point. They are a solubility class of thousands compounds in crude oil which are soluble in aromatics, but are insoluble in n-alkane solvents (Mullins *et al.*, 1998). Different types of n-alkane precipitants used to separate asphaltenes from crude oil exhibit a variation in precipitation power. A quantity of precipitated asphaltenes increases with a decrease in the length of carbon chain of precipitants as seen in Figure 2.1 (Speight, 1999).

Asphaltenes in crude oil are extremely polydisperse contribute to a distribution of molecular weight, heteroatom content and stability (Maqbool *et al.*, 2009). They have an average molecular weight about 750 Da with a variation between 500 and 1000 Da. The Yen-Mullins model, as illustrated in Figure 2.2, is a well-accepted asphaltene architecture which specifies molecular and colloidal structure of asphaltenes in crude oils and laboratory solvents. This model proposed that the asphaltene molecular structure is dominated by the "island" molecular architecture. This molecular architecture consists of one polycyclic aromatic hydrocarbon per molecule surrounded by alkyl chains. At a sufficient concentration, asphaltene

molecules form nanoaggregates with small aggregation numbers and with one disordered stack of aromatics. At higher concentrations, nanoaggregates form clusters (Mullins *et al.*, 2012).

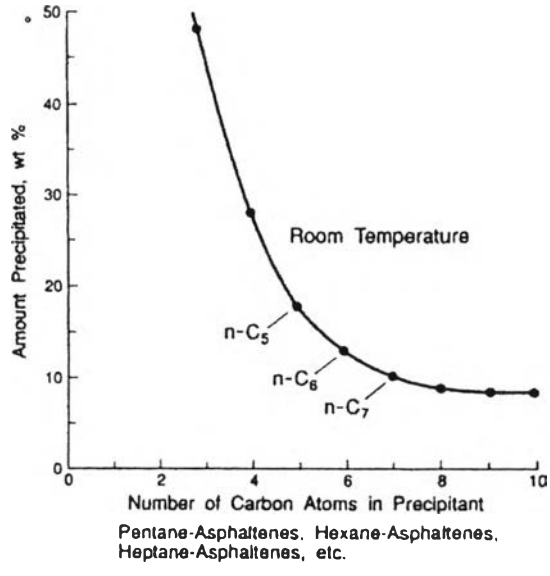

Figure 2.1 Variation of asphaltene yield with n-alkane solvent (Speight, 1999).

Figure 2.2 Yen-Mullins model shows the dominant "island" molecular architecture (Mullins *et al.*, 2012).

The results of asphaltene elemental analysis show that besides carbon and hydrogen asphaltenes contain heteroatoms such as nitrogen, sulfur and oxygen. Moreover, they also contain trace amount of metals such as vanadium and nickel. The elemental composition on the asphaltenes surface resulted from XPS technique

indicates that asphaltenes contain the functional group of carbonyl, hydroxyl and carboxylic. In addition, asphaltenes also consist of thiophenic compound, aliphatic sulfuric compound, pyridinic compound and pyrrolic compound from sulfur and nitrogen (Wang *et al.*, 2009).

2.3 Asphaltene Precipitation

Asphaltene precipitation and deposition are the main problem in oil production of heavy crude oil. Asphaltenes precipitation is not a solubility-driven process but a time dependent phenomenon. The detection time is the time requires for precipitating asphaltenes. It is defined as the time between the onset of haze detection and the onset of precipitation detected under an optical microscope. The detection size of asphaltene particles is about 500 nm. The detection time can actually varies from a few minutes to several months, depending on the precipitant, such as heptane, concentration added to crude oil or model oil. It increases exponentially with decreasing precipitant concentration as presented in Figure 2.3. The asphaltenes with low stability tend to precipitate earlier than the one with high stability at identical precipitant concentration (Maqbool *et al.*, 2009). The asphaltene precipitation is proposed to be occurring because of two asphaltene molecules successfully collide with each other. The collision efficiency of asphaltenes in homogeneous bulk solution is in an order of magnitude of 10^{-6}. The collision efficiency is a parameter showing how many effectively collisions occur from every collision of asphaltene particles (Maqbool *et al.*, 2011). There are soluble and insoluble asphaltenes or, in other word, stable and unstable asphaltenes during precipitation of asphaltenes. After destabilized asphaltenes by adding precipitant, the precipitating unstable asphaltene clusters have a significantly higher fractal dimension compared to the stable ones. Moreover, the unstable asphaltenes particles will significantly increase in size then they are detected under an optical microscope while the stable asphaltenes stay in solution with relatively the same size. The proposed asphaltene precipitation mechanism is shown in Figure 2.4 (Hoepfner *et al.*, 2013).

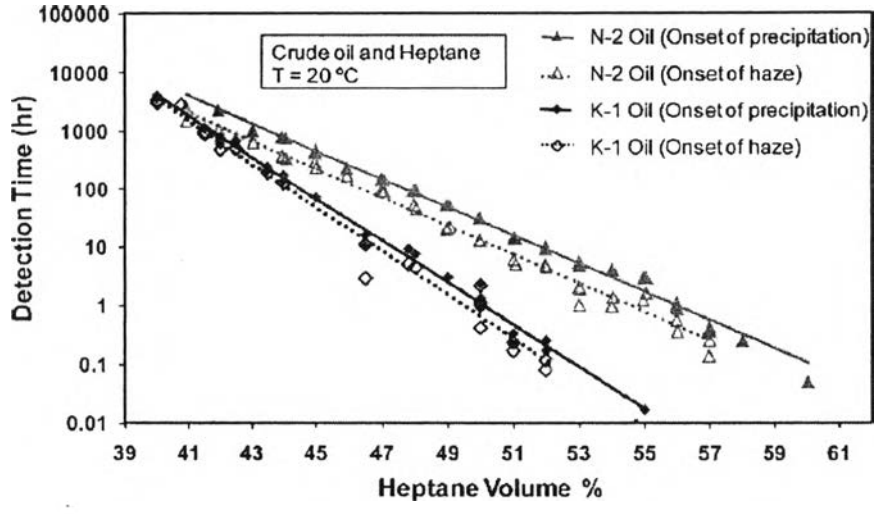

Figure 2.3 Detection time of asphaltene precipitation as a function of precipitant concentration (Maqbool *et al.*, 2009).

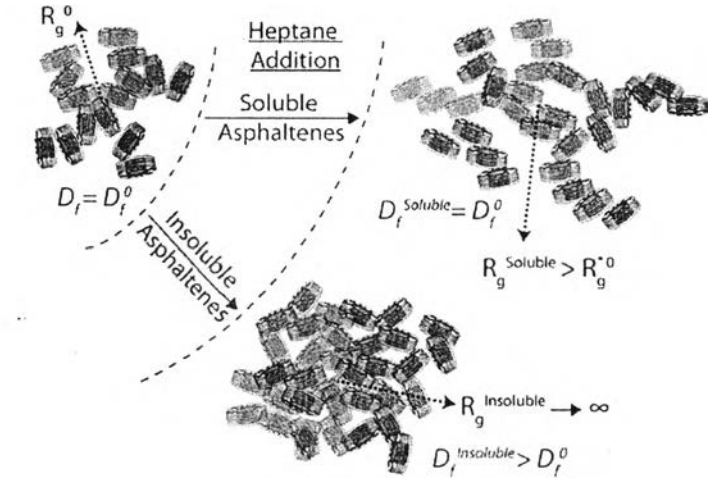

Figure 2.4 Schematic of proposed asphaltene precipitation mechanism. R_g and D_f refer to the radius of gyration and fractal dimension, respectively, of asphaltene fractal clusters in the undiluted crude oil (Hoepfner *et al.*, 2013).

2.4 Interactions of Asphaltenes and Surfaces

The asphaltene deposition is assumedly consist of two step interactions. The first interaction is defined here as adsorption where asphaltenes interact with surface

directly. The second interaction is defined as deposition which occurs when asphaltenes interact with previously deposit asphaltenes on surface. Hence, properties of surface play an important role in asphaltene adsorption. The adsorption capacity is different in each surface materials depending on the size, morphology, porosity, chemical composition, and characteristic of the surface (Adams, 2014). The total bulk surface area will increase if reducing the surface particle size therefore increasing adsorption. Besides the properties of surface, other parameters which affect asphaltene adsorption include chemical characteristic and size of asphaltenes, resins, temperature, and solvent types.

Smoluchowski-Levich approximation was widely used to describe the transport and deposition phenomena of particles in colloidal point of view. This method was approximated base on the irreversible deposition of colloidal particle on surface. The assumptions underlying this method are (a) the interaction of particle and wall is counterbalance by van der Waals attractions and external forces are neglected, (b) the particles move freely in the fluid, and (c) the deposition is independent on interception. The results from this approximation are usually define in term of Sherwood number (Sh) which includes the particle deposition flux. Interestingly, Sh is proportional to Peclet number (Pe) with a power of 1/3 in all investigated geometries in a uniform flow. This dependency is valid for very low Pe (Elimelech et al., 1995).

The free energy for adsorption of asphaltenes from model oil solution can predict the amount of asphaltene adsorption on metals. The free energy prediction shows that asphaltenes preferentially adsorb on gold followed by stainless steel and aluminium (Xie *et al.*, 2005). This prediction is in agreement with experimental results of asphaltene adsorption on metal powder that asphaltenes adsorb mostly on stainless steel powder followed by iron and aluminium powder at equilibrium as shown in Figure 2.5. The adsorption of asphaltenes on stainless steel surface might be influenced by elements in the metal such as chromium, nickel, silicon, and heteroatom which promotes better electrostatic bonding between asphaltenes and stainless steel (Alboudwarej *et al.*, 2005). The adsorption of asphaltenes on glass surface can be quantified by measuring a change of contact angle between asphaltenes and the surface. The asphaltene adsorption increases with decreasing colloidal stability in

model oil solution by adding heptane. It was proved that asphaltenes adsorb on glass through the interaction with silanol group on glass surface (Akhlaq *et al.*, 1997).

The kinetic of asphaltene adsorption is slow and controlled by the diffusion of asphaltenes from bulk solution to the surface (Xie *et al.*, 2005). The size of primary asphaltene molecule and asphaltene aggregate are the two major physical properties of asphaltenes related to asphaltene adsorption. An increase in the aggregate size will decrease the diffusion rate of the aggregates in solution resulting in a decrease in adsorption rate. However, the increasing in size of aggregates increases the total amount of adsorbed asphaltenes on a surface (Adams, 2014). The effect of temperature to asphaltene adsorption is when temperature increases, the amount of asphaltene adsorption at equilibrium decreases. It is likely because of the size of asphaltene aggregates decreases with increasing temperature (Alboudwarej *et al.*, 2005).

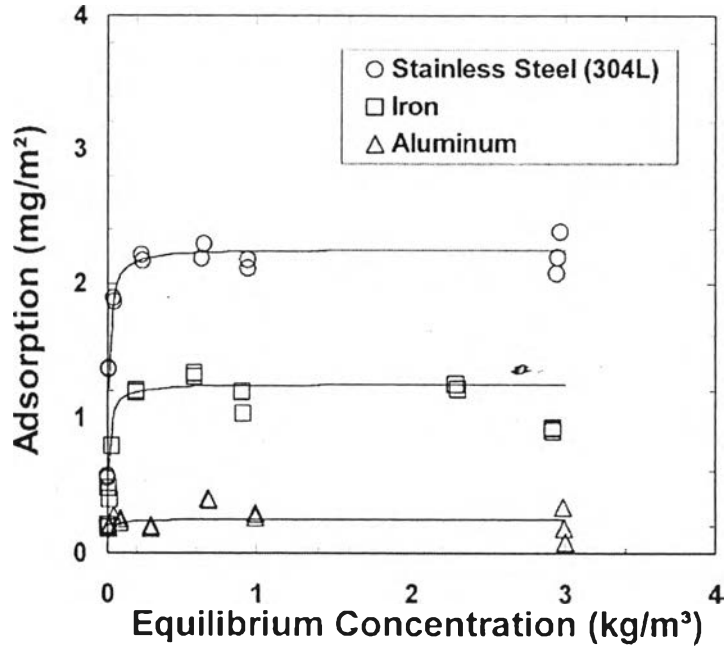

Figure 2.5 Adsorption isotherm for asphaltenes on powdered metals at 22°C (Alboudwarej *et al.*, 2005).

The functional group of adsorbed asphaltenes indicated by XPS consists of carboxylic, pyrrolic, pyridinic, thiophenic, and sulfite (Abdallah *et al.*, 2007). For the adsorption on stainless steel, the amount of heteroatom detected increases when

approaching to the stainless steel surface. This result suggests that a polar interaction of an associated functional group of these heteroatoms is responsible for initiating adsorption (Adams, 2014). This finding is also valid for deposited asphaltenes in the oil field which enrich in heteroatom species, especially oxygen species (Klein *et al.*, 2006). On the other hand, the aromaticity of asphaltenes has been shown to have an important influence on asphaltene adsorption (Adams, 2014). Moreover, there is evidence that deposited asphaltenes from oil field which are believed to be the most unstable asphaltenes contain more metal elements (V, Ni, and Fe) than the asphaltenes extracted from the same crude oil. Furthermore, the high polarity asphaltenes have high tendency to aggregate and deposit in the oil field and hard to remediate (Wattana *et al.*, 2005).

The work from Alboudwarej *et al.* showed that the higher heptane concentration used to destabilize asphaltenes in model solutions, the higher the asphaltenes adsorption (Alboudwarej *et al.*, 2005). Likewise, asphaltene deposition can also occur at low precipitant concentration added to destabilized asphaltenes which there is no asphaltene particles detected under an optical microscope. The asphaltenes only deposit when they are in an aggregating process and the aged asphaltene aggregates which has relatively large aggregate size do not deposit on a surface This result indicates that all the asphaltene deposition is caused by submicrometer aggregates (Eskin *et al.*, 2012; Hoepfner *et al.*, 2013).

2.5 Previous Asphaltene Deposition Investigations and Techniques

Many techniques were used to investigate the effect of asphaltene deposition. Each technique has its benefits and downfalls depending on the aspect of investigation. The quartz crystal microbalance with dissipation measurement was used to study the asphaltene adsorption in different environment conditions. The adsorbed mass was in an order of nanogram. The results indicate that the kinetic of a long adsorption process was control by mass transfer for both model oil and crude oil (Tavakkoli *et al.*, 2013; Tavakkoli *et al.*, 2014). Eskin *et al.* and Akbarzadeh *et al.* used the couette device to simulate the flow condition in the pipeline to investigate asphaltene deposition. The devices have two systems which are batch and flow-through. The results show that the

mass of asphaltene deposit in batch system was clearly lower than the asphaltenes deposited in the flow-through system. This result reveals that the depletion of asphaltenes in solution during an experiment in a batch system has a major effect to asphaltene deposition then leads to the underestimation of the deposition rate. Moreover, the asphaltene deposition rate is highly depend on wall shear stress as presented in Figure 2.6 where the asphaltene deposition rate decreases with increasing wall shear stress (Akbarzadeh *et al.*, 2010; Eskin *et al.*, 2012).

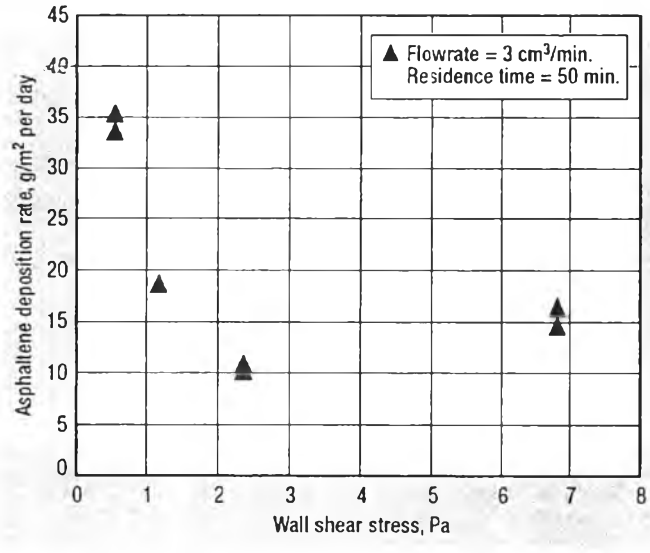

Figure 2.6 The effect of wall shear stress on asphaltene deposition rate (Akbarzadeh *et al.*, 2010).

The capillary technique is widely used for studying the asphaltene deposition because it clearly demonstrates the flow in a pipeline (Wang *et al.*, 2004; Boek *et al.*, 2008; Nabzar *et al.*, 2008; Hoepfner *et al.*, 2013). The asphaltene deposition in capillary tube was detected by pressure drop between the inlet and the outlet of the capillary. The deposition rate is increased with an increase in precipitant concentration as presented in Figure 2.7. However, the mass of the deposit in a capillary tube is too small to collect for further characterization and this technique is also very difficult to measure the asphaltene deposition rate. In addition, the very small diameter of stainless steel capillary tube generates a high shear rate inside the capillary from the flow which

is likely to be the cause of the deposit sloughing off the wall and the visual investigation of the deposit can only be observed at the inlet and the outlet of the capillary by SEM (Hoepfner *et al.*, 2013). The rectangular glass microcapillary was used to observe the deposition behavior of the asphaltenes as showed in Figure 2.8. It was observed that the deposits started to build up and accumulated then they were entrained by the flow. This visual observation was in a good agreement with the pressure drop results (Boek *et al.*, 2008). Another evidence of shear rate hinder the asphaltene deposition is showed by Nabzar *et al.* as presented in Figure 2.9. The shear rate can be increased by either increasing the flow rate or decreasing the diameter of the capillary which could imply to the diameter of the pipeline or the pore size of the porous oil reservoir (Nabzar *et al.*, 2008).

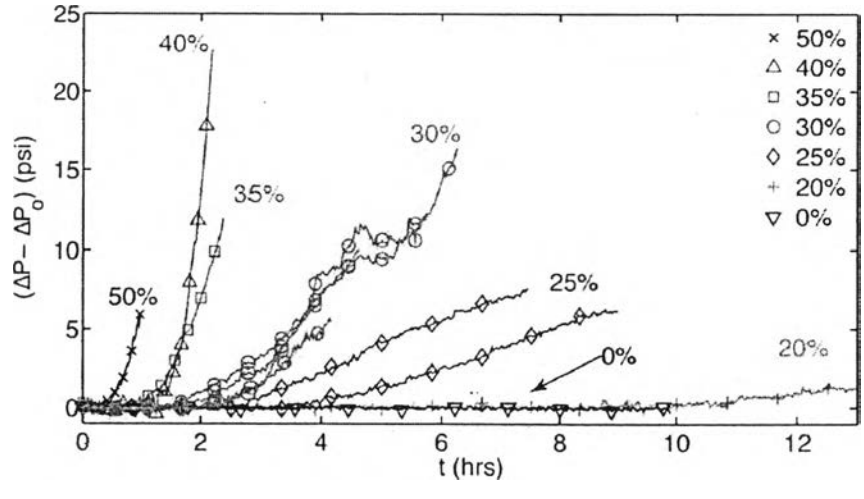

Figure 2.7 Pressure drop as a function of time for crude oil with various heptane volume percent (Hoepfner *et al.*, 2013).

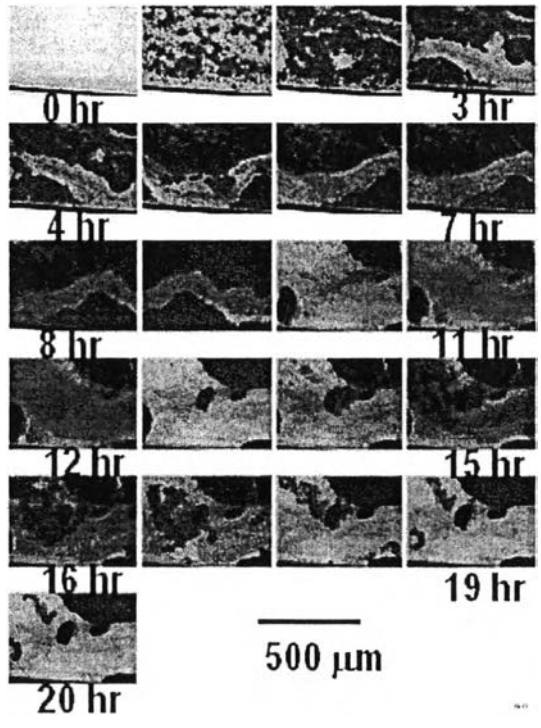

Figure 2.8 Images of asphaltene deposition in rectangular glass microcapillary (Boek *et al.*, 2008).

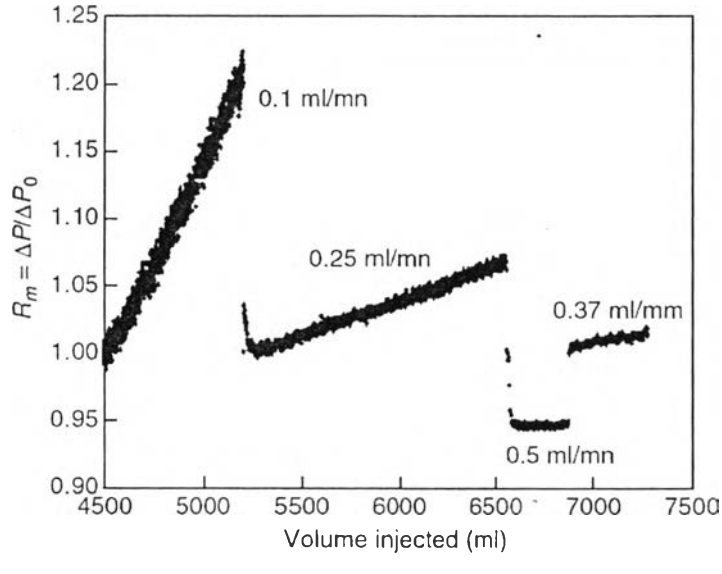

Figure 2.9 The evidence of shear limitation in asphaltene deposition (Nabzar *et al.*, 2008).

The transparent packed-bed micro-reactor with an accurate control condition developed and used by Hu *et al.* has a very good characteristic for visual inspection. The packed-bed micro-reactor was packed with quartz micro-particle with the mean particle size of 29 micrometer. The amount of asphaltene deposits decrease with increasing in Reynolds number. The asphaltene adsorption was observed only at low Reynolds number in the packed-bed micro-reactor. However, the asphaltene deposit at high Reynolds numbers was because of mechanical entrapment which likely due to the very small pore size of the packed-bed (Hu, 2014).

There are many factors to take into consideration in order to design a better apparatus to investigate asphaltene deposition and approach the mechanism of asphaltene deposition in flow condition by asphaltene adhesion or attachment onto the surface. Firstly, the size of an apparatus has to be large enough to provide an adequate surface area for capturing great amount of deposit for further characterize the properties of the deposited asphaltenes. Secondly, the apparatus should be transparent to be able to have a visual inspection of the deposited asphaltenes. Thirdly, the apparatus should not generate high shear rate. Fourthly, the deposition in the apparatus has to cause by adhesion of asphaltene particle in order to be able to investigate the interaction of asphaltenes and surface and also the effect of the hydrodynamics of the flow. Fifthly, the concentration of asphaltenes in a testing oil solution has to be kept as constant as possible to avoid the effect of asphaltene depletion. Lastly, the asphaltene deposition rate has to be able to measure from the apparatus.

2.6 Packed-bed Characterization and Flow Properties

The fluid flow pattern in packed-bed is more complicated than the flow pattern in a pipeline. Therefore, many parameters is calculated and measured in order to characterize a packed-bed. Porosity (ϕ) and permeability (κ) are two significant parameters to characterize the porous media in a packed-bed. Porosity or void fraction is a parameter describes how much the void space is in a porous media. It can be obtained from the ratio of the volume of the void in pack-bed, V_V, and the total volume of a packed-bed, V_T.

$$\phi = \frac{V_V}{V_T} \tag{2.1}$$

Permeability expresses the ability of the porous media to allow the fluid to flow through. Permeability can be simply obtained from Darcy's Law which describes the fluid flow through the porous media (Hu et al., 2014).

$$\kappa = \frac{\mu Q}{A}\frac{L}{\Delta P} \tag{2.2}$$

where μ is the dynamic viscosity of the fluid, Q is the volumetric flow rate of the fluid, A is the cross-sectional area of the column perpendicular to the direction of the flow, L is the bed length, and ΔP is the pressure drop across the packed-bed.

The superficial velocity is a hypothetical velocity that is usually measured for the flow in a porous media. It is equivalent to the velocity of the flow in an empty tube. The superficial velocity can be expressed as,

$$u = \frac{Q}{A} \tag{2.3}$$

However, the actual fluid velocity within the packed-bed will be greater than the superficial velocity. This velocity is so called interstitial velocity, u_i, which can be obtained by,

$$u_i = \frac{u}{\phi} \tag{2.4}$$

Other important parameter to be measured is Reynolds number (Re) in order to distinguish the flow regime of the fluid in a packed-bed. Re in a packed-bed can be determined by,

$$Re = \frac{d_p u \rho}{(1-\phi)\mu} \tag{2.5}$$

where d_p is the mean particle size and ρ is the density of the fluid. In a packed-bed, the fully laminar exists for Re □10, while fully turbulent when Re □2000 (Hu et al., 2014).

The pressure of the fluid will decrease due to friction when flowing through a packed-bed column. The pressure drop across a packed-bed can be calculated from Ergun's equation. Ergun's equation additively combines the laminar and turbulent components of the pressure gradient (Rhodes, 2008). This equation is expressed as,

$$\frac{-(\Delta P)}{L} = 150\frac{\mu u}{d_p^2}\frac{(1-\phi)^2}{\phi^3} + 1.75\frac{\rho u^2}{d_p}\frac{(1-\phi)}{\phi^3} \tag{2.6}$$

Thoenes and Kramers have investigated the mass transfer coefficient for the fluids flowing in packed-bed with different packing geometries (Thoenes et al., 1957). The results of all investigated fluids and packing patterns follow a correlation between Sh, Re and Schmidt number (Sc). The dependency of Sc on Sh is scale with the power of 1/3. The flow in a packed-bed is never completely laminar or fully turbulent as a consequence of complexity of the flow pattern in a packed-bed. A particular part of surface could be exposed to a turbulent flow, while in a narrow edge of the surface experiences the laminar flow. Hence, the dependency of Re on Sh is changes with the flow regime where Sh α $Re^{0.2}$ in a stagnant regime, Sh α $Re^{1/3}$ in a laminar regime, and Sh α $Re^{0.8}$ in a turbulent regime. Finally, a correlation for mass transfer coefficient for a packed-bed which contribute to both laminar and turbulent convective transfer as well as diffusion in a stagnant region was proposed and expressed by the following equation,

$$Sh = 1.0Re^{1/2}Sc^{1/3} \tag{2.7}$$

This correlation can be used with the mean deviation for 10% only. Therefore, the mass-transfer flux, J, is proportional to the superficial velocity by,

$$J \alpha u^{1/2} \tag{2.8}$$

The diffusivity (D) can be obtained from Thoenes and Kramers correlation for packed-bed. Moreover, the size of diffused particle can also be estimated from the diffusivity by using Stokes-Einstein equation (Miller, 1924). This equation is valid for a diffusion of spherical particles through a liquid at low Reynolds number which is expressed by,

$$D = \frac{k_B T}{6\pi\mu r} \tag{2.9}$$

where k_B is Boltzmann's constant, T is the absolute temperature, and r is the radius of the spherical particle.